

Time-Scale Dependencies for Image Compression

V. Bruni, B. Piccoli, D. Vitulano

Istituto per le Applicazioni del Calcolo "M. Picone" C.N.R.

Viale del Policlinico, 137 00161 Rome, Italy

{bruni, piccoli, vitulano}@iac.rm.cnr.it

Abstract—The definition of an atomic representation of the wavelet transform of a signal allows us to write the evolution law through scales for modulus maxima of the transform. Although this result is very general and useful for various fields of image processing, we focus on its application to signal and image compression. We propose a simple trick for taking advantage from the law without directly solving its corresponding partial differential equation. Preliminary experimental results show that the proposed approach outperforms available compression techniques.

Index Terms—Wavelet Transform, Time-Scale Dependencies, Image Compression, Sparse Representation.

I. INTRODUCTION

Sparse representation is a key point in many fields of Image and Signal Processing. The aim is often reached by providing a transform which carries the main structures of the analysed image or signal. Wavelet bases well attain this task since they work like differential operators at different resolutions. Moreover, in [7], [8] it has been proved that the amplitude of wavelet coefficients across scales depends on signal regularity, i.e. its Lipschitz order. In particular, for a restricted class of wavelet functions, the right evolution law of modulus maxima can be computed [7]. This property allows to eliminate *interscale redundancies*. Nonetheless, for complicated signals it could be difficult to estimate the right Lipschitz order. In fact, singularities overlap and the computational effort of the corresponding algorithm increases, resulting somehow unuseful in various applications, such as image compression. The most efficient wavelet based coding techniques, such as EZW [12], SPIHT [11], JPEG2000 [13], try to overcome this problem by empirically exploiting a *parent-child* relationship between coefficients belonging to different scale levels — for each high amplitude coefficient at the coarsest scale there exists a high amplitude coefficient in the same position at finer scales, with high probability [12]. A further effort for giving a precise rule for chaining wavelet coefficients has been made in [5]. The authors focused on a restricted class of signals and defined space-scale vectors, called *footprints*, which

consist of wavelet coefficients generated by singularities of piecewise polynomial signals. They provide an exact reconstruction of piecewise polynomial signals and a suitable approximation of piecewise smooth functions. Nonetheless, a *footprints* decomposition strongly depends on the distance between the closest singularities of the analysed signal, since it has some difficulties in separating the contribution of overlapping singularities.

In [2], [4], the authors proposed to model wavelet bands as travelling waves which dilate and interfere through scales. Each wave represents a singularity point in the original signal and the interference of two or more of them can be modelled exploiting the *overlapping effects principle* in the wavelet domain. To reduce the computational effort, a single waveform (atom) is used. Each atom is characterized by the location and the amplitude of its modulus maximum and corresponds to an *infinite ramp* signal in the spatial domain, as depicted in Fig. 1b. The amplitude of modulus maximum is proportional to the ramp slope α_0 . This choice allows a representation by maxima of the wavelet transform and the nice symmetric shape of the atom is helpful in managing interfering waves. More complicated signals are then approximated using 1^{st} order polynomial functions around each singularity point. Even though this approximation is more rough than the one of *footprints*, it allows us to manage interfering singularities with a simple and fast algorithm (*WISDOW*) which works at each scale independently. Therefore, it is able to provide a somewhat faithful approximation of a large class of signals, as shown in [4].

In this paper a step forward has been done. Taking advantage of the atomic decomposition, the evolution law through scales of wavelet modulus maxima is written and a precise rule for constructing maxima chains along scales is derived. It is proved that wavelet detail bands are the solution, at a fixed scale, of a first order partial differential equation (PDE). It enables to derive significant modulus maxima locations as the solution of an ordinary differential equation (ODE) with suitable initial conditions. Hence, the law allows us to reconstruct wavelet detail bands at successive scale levels just from the atoms of the first level. It is worth outlining that the law gives the wavelet transform at any scale and then

⁹Based on "Wavelet Time-Scale Dependencies for Signal and Image Compression", by V. Bruni, B. Piccoli, D. Vitulano, which appeared in the Proceedings of the 4th International Symposium on Image and Signal Processing and Analysis, Zagreb, Croatia, September 2005. 2005 IEEE.

it is able to also model interfering waves (singularities whose distance is smaller than the wavelet support at a fixed scale level). In other words, it is not necessary to constrain the distance between two singularity points for reconstructing the original signal, as in [5].

The law is not well adaptable to multi-resolution. In fact, it cannot include decimators since they do not guarantee a unique and continuous maxima chain along scales. Therefore, it can be used in the continuous wavelet transform domain or in an overcomplete discrete wavelet decomposition. The redundancy of an overcomplete decomposition can be compensated by the sparseness of the atomic representation, as it will be clearer in the following. The law concerns 1D signals, since the atomic representation has been defined for one dimension. In 2D case it is necessary to split the image into independent 1D signals (rows, columns or anything else) and separately process each of them.

As previously seen, it is possible to reconstruct the original signal from wavelet atoms at first scale and the approximation at the coarsest scale. The starting conditions consist of locations of atoms maxima, their amplitude and their growing law too (Lipschitz regularity). It turns out that the law cannot be directly used in image coding since it requires too much information to code along with an intensive computational effort for solving the PDE. In this paper we try to overcome this difficulties by solving the law one step at a time, from coarser to finer scales. Taking advantage of the atomic representation of detail bands, we get an estimate of atoms maxima locations and their corresponding slopes. Then we exploit relations between low and high pass components of an over-complete representation of the signal. This is possible thanks to the frequency intersection of analysis and synthesis filters of the decomposition. Experimental results outperform wavelet based coding techniques and standard JPEG [1] and JPEG2000 [13], even in a non optimized numerical scheme.

The outline of the paper is the following. Section II briefly presents the atomic representation and a modified expansion algorithm. In Section III atoms evolution law is provided and its adaptation to image compression is described in Section IV. In Section V some preliminary experimental results are shown. Finally, discussions and conclusions are drawn in Section VI.

II. THE ATOMIC REPRESENTATION

Let f be an infinite ramp signal, as the one depicted in Fig. 1a, having the singularity located at t_0 with slope α_0 . It can be analytically represented as

$$f(t) = \beta_0 \chi_{(-\infty, t_0]}(t) + [\alpha_0(t - t_0) + \beta_0] \chi_{[t_0, +\infty)}(t). \quad (1)$$

Let $Wf(u, s)$ be its wavelet transform at time u and scale s using the mother wavelet function ψ , whose support is the interval $[a, b]$, that is

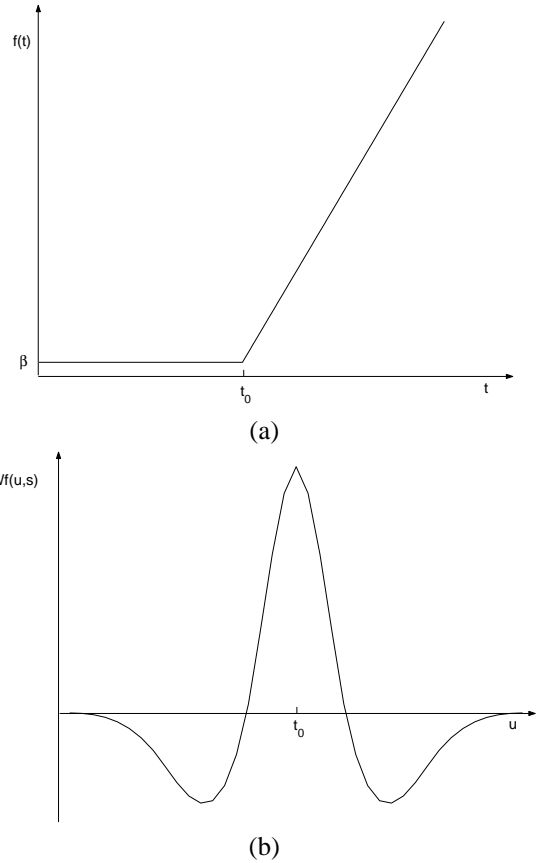


Fig. 1. **a)** Infinite ramp signal having a singularity point at location t_0 . **b)** Basic atom (eq. (3)) computed at a fixed scale s and using the spline biorthogonal wavelet 3/9 [7]. It corresponds to the wavelet transform of the infinite ramp signal.

$$Wf(u, s) = \frac{1}{\sqrt{s}} \int_{u+sa}^{u+sb} f(t) \psi^* \left(\frac{t-u}{s} \right) dt = \alpha_0 s \sqrt{s} \left(\int_{\frac{t_0-u}{s}}^b t \psi(t) dt - \frac{t_0-u}{s} \int_{\frac{t_0-u}{s}}^b \psi(t) dt \right). \quad (2)$$

We define as *basic atom* at scale s and centered at the location t_0 , the following function

$$F(t_0, u, s) = s \sqrt{s} \left(\int_{\frac{t_0-u}{s}}^b t \psi(t) dt - \frac{t_0-u}{s} \int_{\frac{t_0-u}{s}}^b \psi(t) dt \right), \quad (3)$$

The atom shape is depicted in Fig. 1b, where a spline biorthogonal wavelet has been employed¹.

Therefore, $Wf(u, s)$ in eq. (2) is composed of a basic atom centered at t_0 with amplitude α_0 .

Let us now investigate signals with more than one singularity point. Figs. 2 and 3 represent two signals having two singularity points and their corresponding wavelet transforms. Each of them shows two atoms which independently grow and dilate till they begin to overlap (see $s = \bar{s} = s_3$ in Fig. 2 and $s = \bar{s} = s_4$ in Fig. 3). We

¹This wavelet has been selected only for academical purposes. In fact, it is symmetric, compactly supported and it has a closed form [7].

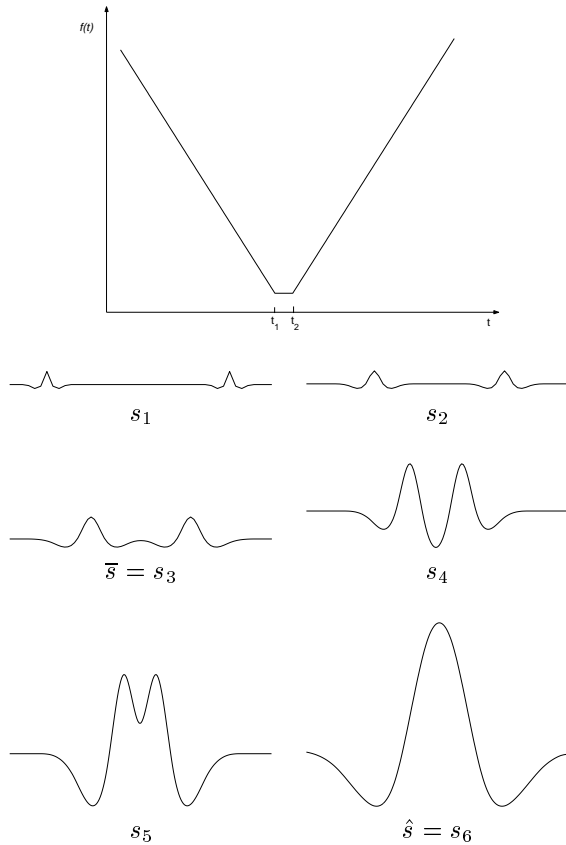


Fig. 2. Topmost figure depicts a signal having two singularity points at t_1 and t_2 . Below there is its corresponding wavelet transform computed at successive scales $s = \{s_1, \dots, s_6\}$. It is composed of two atoms having the same sign which interfere as long as the scale increases.

can say that from scale \bar{s} the atoms become to interfere till they completely merge (see scale $s = \hat{s} = s_6$ in Fig. 2 and $s = \hat{s} = s_6$ in Fig. 3). From this point on ($s > \hat{s}$), the shape of interfering atoms does not change while it still grows and dilates. Moreover, if the atoms have the same sign, they converge to a single atom. On the other hand, if the atoms have an opposite sign (Fig. 3), they approach a wave which is characterized by two symmetric mainlobes having opposite sign. Furthermore, *piecewise constant signals* can be modelled as the composition of two or more infinite ramp signals. For example, the wavelet transform of a step function is the superimposition of two interfering basic atoms at locations t_1 and t_2 , when t_2 approaches t_1 , as proved in the Appendix A.

The wavelet transform of polynomial ramps can be approximated by a symmetric basic atom and a residual. The latter is negligible if the terms of order greater than one in a linear approximation of $f(t)$ around the singularity location are negligible with respect to the wavelet support S_ψ . Whenever the error increases, the atom shape can be modelled as the superimposition of two or more adjacent atoms. Therefore, piecewise polynomial signals can be represented as interfering basic atoms in the scale space wavelet domain — see [4] for details.

More in general, the *overlapping effects principle* can

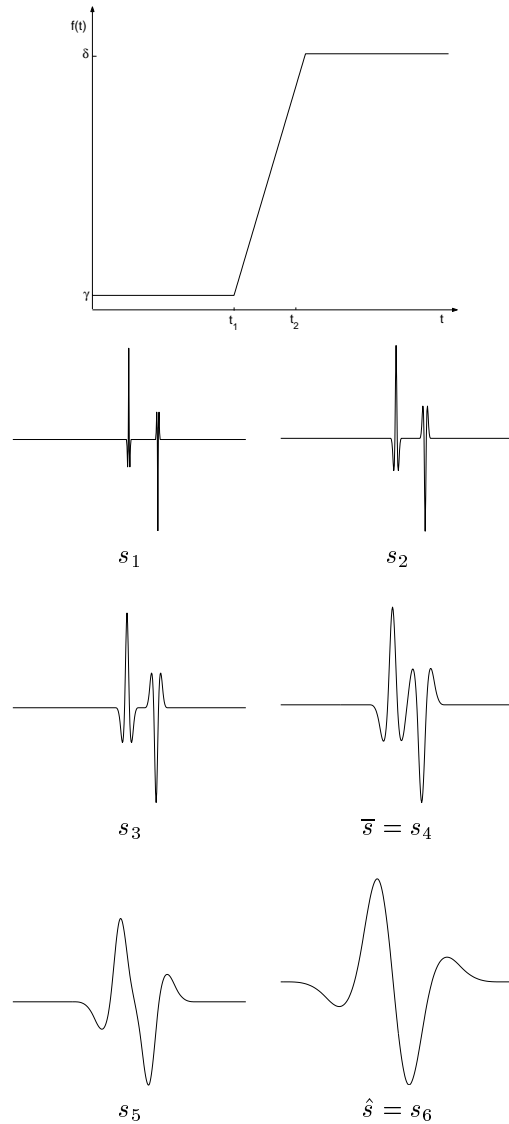


Fig. 3. Topmost figure depicts a signal having two singularity points at t_1 and t_2 . Below there is its corresponding wavelet transform computed at successive scales $s = \{s_1, \dots, s_6\}$. It is composed of two atoms having opposite sign which interfere as long as the scale increases.

be independently applied at each scale of the wavelet transform $Wf(u, s)$. Therefore, it is always possible to provide a representation by atoms of a generic signal f , that is

$$\forall s > 0, \quad Wf(u, s) \approx \sum_{k=1}^{N_s} \alpha_k F(t_k, u, s),$$

where α_k and t_k are respectively the slope and the location of each atom of the representation, while N_s is the number of the atoms used for the approximation at scale s .

It is worth outlining that this model allows us to drastically reduce the information which is necessary for reconstructing the original signal. In fact, it consists of atoms locations t_k and their slopes α_k at each scale s . These two parameters contain information about the value of the wavelet transform of the signal at scale s

within the support of the atom centered at t_k . Hence, it intrinsically preserves the correlation between adjacent coefficients of the wavelet decomposition without having a priori information about the analysed signal (see Figs 2 and 3). This is a crucial requirement for a successful compression scheme.

In the following section, we provide a fast and effective algorithm for the computation of the slope and the location of each atom of the decomposition.

A. Atoms estimation

The expansion of a generic signal f into a finite number of atoms requires the knowledge of their location. Each atom can be characterized by its modulus maximum, as arises from Fig.1b. Therefore, local extrema of the wavelet transform of the signal f can guide in the search of atoms locations $\{t_k\}_{1 \leq k \leq N_s}$ at each scale s .

In [4], a greedy strategy has been employed. The algorithm works like a *matching pursuit* [9], when the rule for selecting the atom in the adopted dictionary is the amplitude of the modulus maximum of the wavelet transform at a fixed scale s . More precisely, at each scale s , the most important modulus maximum of $Wf(u, s)$ is selected. Hence, an atom centered at the found location t_1 is considered and its slope α_1 is estimated in the interval $[t_1 - sb, t_1 - sa]$ as the inner product

$$\alpha_1 = \frac{\langle Wf(u, s), F(t_1, u, s) \rangle}{\|F(t_1, u, s)\|^2}.$$

If $R_1(u, s) = Wf(u, s) - \alpha_1 F(t_1, u, s)$ is the residual, the successive atom is estimated from $R_1(u, s)$ in the same way, i.e. $\alpha_2 = \frac{\langle R_1(u, s), F(t_2, u, s) \rangle}{\|F(t_2, u, s)\|^2}$ and a new residual $R_2(u, s) = R_1(u, s) - \alpha_2 F(t_2, u, s)$, is computed. The estimation of the k^{th} atom gives $R_k(u, s) = R_{k-1}(u, s) - \alpha_k F(t_k, u, s)$, where $\alpha_k = \frac{1}{\|F(t_k, u, s)\|^2} \langle R_{k-1}(u, s), F(t_k, u, s) \rangle$.

The iterations stop when we have no more significant maxima, i.e. their energy is lower than a prefixed tolerance. The following atomic approximation is then provided

$$\tilde{W}f(u, s) = \sum_k \alpha_k F(t_k, u, s).$$

Fig. 4 depicts the atoms representation of a signal which is achieved using the algorithm described above.

At each iteration k , the approximation error is:

$$\begin{aligned} \epsilon(u, s) &= Wf(u, s) - \tilde{W}f(u, s) = \\ &= Wf(u, s) - \sum_{h=1}^k \frac{\langle Wf(u, s), F(t_h, u, s) \rangle}{\|F(t_h, u, s)\|^2} F(t_h, u, s) + \\ &- \sum_{h=1}^k \frac{\sum_{l=1}^{h-1} \alpha_l \langle F(t_l, u, s), F(t_h, u, s) \rangle}{\|F(t_h, u, s)\|^2} F(t_h, u, s). \end{aligned}$$

It is composed of two terms. The first one, i.e.

$$Wf(u, s) - \sum_{h=1}^k \frac{\langle Wf(u, s), F(t_h, u, s) \rangle}{\|F(t_h, u, s)\|^2} F(t_h, u, s)$$

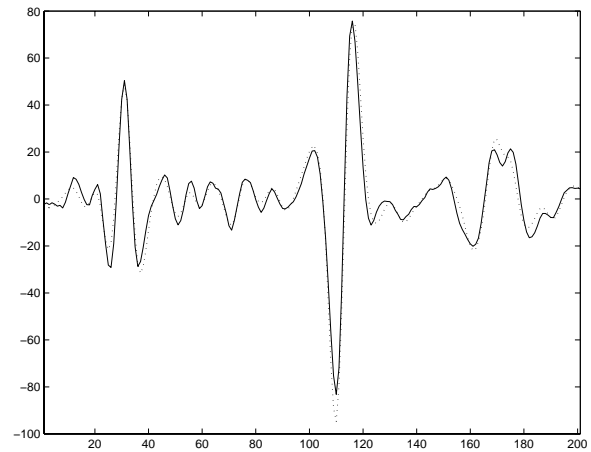


Fig. 4. a) Zoom of the wavelet transform at $s = 2^3$ (solid) of row no. 100 of $512 \times 512 \times 8$ bits of Lena image and its corresponding atoms based approximation (dotted). Atoms are estimated using the Algorithm in [4]. The recovered signal yields MSE (Mean Square Error) = 2.16.

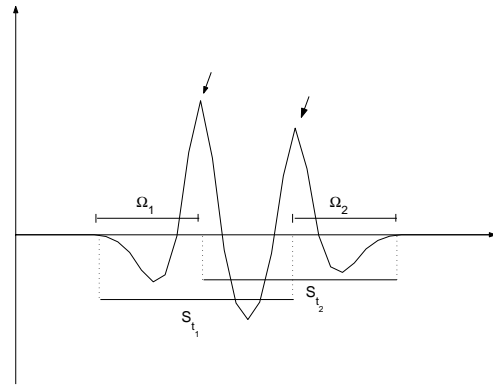


Fig. 5. Two interfering atom before they completely merge. The coefficients in the interval Ω_1 are only relative to the atom located at t_1 while the domain Ω_2 only contains information about the atom at t_2 . Atoms at t_1 and t_2 are respectively indicated by the left and right arrows.

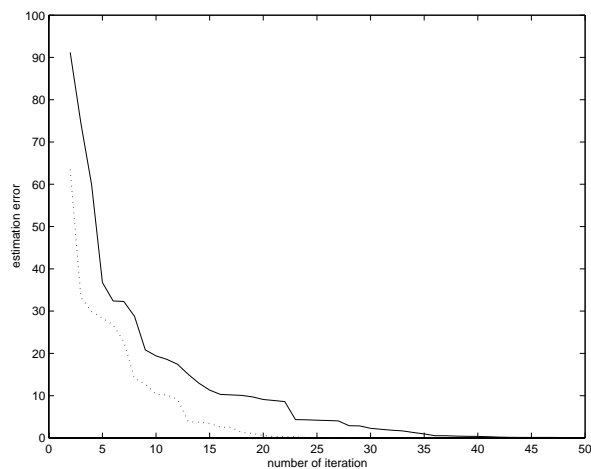


Fig. 6. Atoms estimation error (in terms of MSE) versus number of iterations for the 3^{rd} scale level of row no. 300 of Lena image: matching pursuit based algorithm in [4](solid line), left-right algorithm proposed in this paper (dotted line).

is related to the fitting of the data, and then to the ability of the atom in approximating the shape of the wavelet transform in the considered range. The second one takes into account the interference with eventual neighbouring atoms. It is obvious that the closer the atoms the more significant is the selection of the domain for the estimation of their slopes — the more sensitive is the last term of $\epsilon(u, s)$.

The latter can be minimized at each iteration if a different strategy is adopted. The aim is to estimate the domain Ω_k which is only influenced by the atom centered at t_k (see Fig. 5) such that the estimation

$$\alpha_k = \frac{\langle R_{k-1}(u, s), F(t_k, u, s) \rangle_{\Omega_k}}{\|F(t_k, u, s)\|_{\Omega_k}^2} \quad (4)$$

gives the minimum distortion. In this case, we force the second term of $\epsilon(u, s)$ to approach zero at each iteration. It turns out that the only contribution in the error $\epsilon(u, s)$ is the one of the atomic representation. In fact, at each scale s , for $0 < |t_i - t_j| \leq (b - a)s$, the support of the two interfering atoms do not completely overlap. Hence, it is still possible to distinguish the contribution of each atom. Let S_{t_i} and S_{t_j} respectively be the support of the atoms centered at locations t_i and t_j at a fixed scale s : $S_{t_i} = [t_i - bs, t_i - as]$ and $S_{t_j} = [t_j - bs, t_j - as]$. Then, $\exists \Omega_i, \Omega_j$ such that $\Omega_i \cap \Omega_j = \emptyset$ and $\Omega_i \cup \Omega_j = (S_{t_i} \cup S_{t_j}) - (S_{t_i} \cap S_{t_j})$. The domain Ω_i only contains the contribution of the atom at t_i , vice versa for Ω_j , as depicted Fig. 5. In that way, the estimation error for atoms weights approaches zero.

Therefore, instead of estimating atoms for decreasing energy, as done in the previous algorithm, they can be selected with respect to their location (for example from the left to the right or viceversa).

If we decide to go from left to right, we are interested in finding the leftmost sidelobe of the atom, since it is less influenced by the next one. Once its contribution is computed, it is subtracted from the signal. Hence, the estimation of the next atom can be performed on the residual signal and so on. In that way, at each iteration we minimize the errors due to $\alpha_k s$ estimation in the case of significant interference. In Fig. 6 the decay of the approximation error for the two algorithms is depicted while in Fig. 7 the same signal of Fig. 4 has been approximated using the aforementioned algorithm. It can be noticed that this latter is more precise, yielding a lower mean square error.

In the following we briefly give the detailed algorithm.

The Algorithm

Let us consider the wavelet transform [7] $Wf(u, s)$ of a signal f . Let $\tilde{W}f(u, s)$ its atomic decomposition, which is initialized to zero, and $R_0(u, s) = Wf(u, s)$ the residual. Hence, for each scale s :

- 1) Compute modulus maxima $\{m_h\}_{1 \leq h \leq \overline{N}_s}$.
- 2) Be $M = \{m_h\}_{1 \leq h \leq \overline{N}_s}$. Sort M in increasing (or decreasing) order with respect to their location.

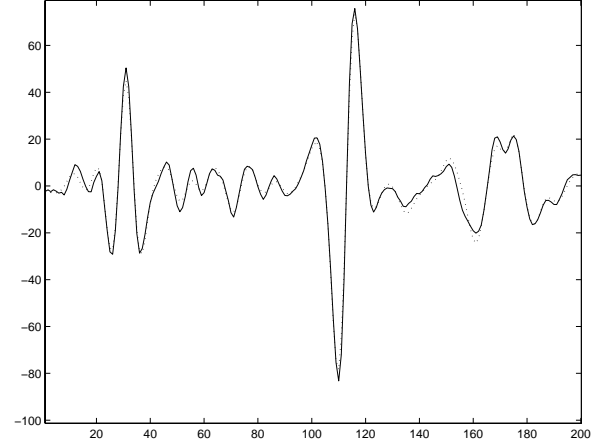


Fig. 7. a) Zoom of the wavelet transform at $s = 2^3$ (solid) of row no. 100 of $512 \times 512 \times 8$ bits of Lena image and the corresponding atoms based approximation (dotted). Atoms are estimated using the Algorithm described in the text. The recovered signal yields MSE = 1.67.

3) Put $k = 1$. For each $m_h \in M$:

- if $|m_h - m_{h+1}| > |b - a|s/2$, the maximum is isolated.

Put $t_k = m_h$.

Estimate the coefficient α_k in domain S_{t_k} :

$$\alpha_k = \frac{\langle R_{k-1}(u, s), F(t_k, u, s) \rangle_{S_{t_k}}}{\|F(t_k, u, s)\|_{S_{t_k}}^2};$$

- else the maximum is not isolated and it is a sidelobe. Let d_k be the distance between mainlobe and sidelobe of the basic atom.

Put $t_k = m_h + d_k$ and estimate α_k in the least square sense in the interval $\Omega_k = [m_h - d_k, m_h]$;

- model the atom centered at t_k in its support S_{t_k} , i.e.

$$\alpha_k F(t_k, u, s), \quad t_k - bs \leq u \leq t_k - as;$$

- add the estimated atom to $\tilde{W}f(u, s)$ and subtract it from the residual $R_{k-1}(u, s)$, i.e. $\forall u$: $t_k - bs \leq u \leq t_k - as$

$$\tilde{W}f(u, s) = \tilde{W}f(u, s) + \alpha_k F(t_k, u, s),$$

$$R_k(u, s) = R_{k-1}(u, s) - \alpha_k F(t_k, u, s).$$

- Put $k = k + 1$.

4) Invert the transform $\tilde{W}f(u, s)$.

III. ATOMS EVOLUTION THROUGH SCALES

In the previous section the atomic decomposition has been used for approximating the wavelet transform $Wf(u, s)$ of a generic function f at each scale independently. Nonetheless, $Wf(u, s)$ reveals an intrinsic time-scale structure, as shown in Fig. 8. In fact, there is a precise link between modulus maxima at successive scales. Nonetheless, it is difficult to build the modulus maxima chains along scales in a deterministic way; modulus maxima can change their locations and they can assume different appearance whenever the cones of influence of two singularities intersect. For that reason,

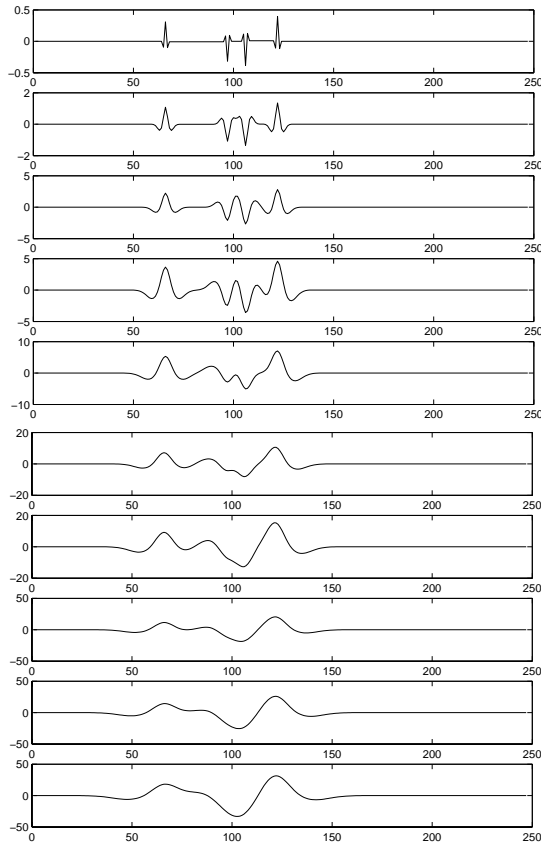


Fig. 8. Wavelet transform computed up to scale $s = 10$ of a signal having four singularity points.

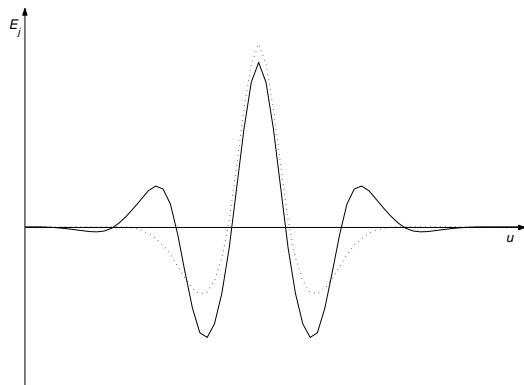


Fig. 9. Shape of the basic atom for the error E_J (solid line). Shape of the true basic atom of the detail band D_J (dotted line), as in Fig. 1b.

some empirical constraints have been used for building the chain, such as the persistency of the sign and the definition of one global maximum in the cone of influence of each singularity [8], [10]. This leads to some false alarms or the missing of important information.

The main contribution of this section consists of providing the trajectories of significant modulus maxima of $Wf(u, s)$ in a theoretical and almost precise manner. These trajectories model the evolution law of predefined basic atoms whose superimposition approximates $Wf(u, s)$. For each atom, the significant maximum is the one having the greatest amplitude (see Fig. 1b) and

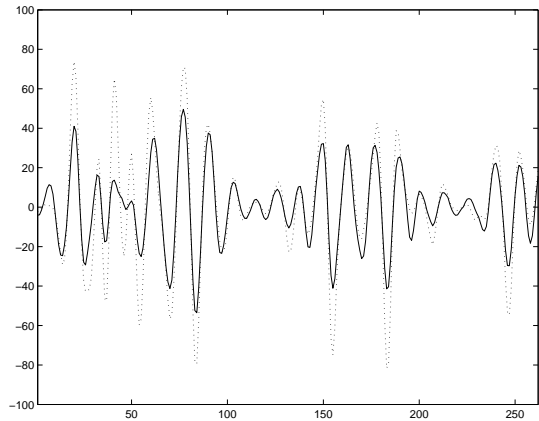


Fig. 10. Zoomed error E_J (solid line) computed for detail band at 3^{rd} level (dotted line) of column no. 100 of Lena image.

it does not disappear along scales but it moves from its initial location whenever its relative atom interferes with an adjacent one. In the case of complete interference the two atoms can generate an only one maximum which takes into account both contributions (see Fig. 2). Using this representation, we can say that significant modulus maxima characterize the atomic decomposition of the wavelet transform. Notice that the latter gives only an approximation of a signal and not its perfect reconstruction.

As shown in Appendix B, it is necessary to have further information about the signal f for writing a really useful partial differential equation for its wavelet transform. In particular, if f is the infinite ramp signal in eq. (1), its wavelet transform at time u and scale s is

$$Wf(u, s) = \alpha_0 F(t_0, u, s).$$

Hence, the evolution law through scales of a single basic atom is:

$$\frac{\partial}{\partial s} Wf(u, s) = \frac{t_0 - u}{s} \frac{\partial}{\partial u} Wf(u, s) + \frac{3}{2s} Wf(u, s). \quad (5)$$

(see eq. (13) in the Appendix B).

In the Appendix B it is also shown how it is possible to derive the equation regulating just the modulus maximum location of the atom (eq. (18)). It turns out that for a single atom, the maximum location does not change along scale levels. A similar equation can be derived for overlapping atoms (see eq. (19)). In this case, maxima locations can shift along scales since corresponding waves interfere. To highlight this point, the equation for two interfering atoms is given

$$\dot{u} = -\frac{\bar{t} - u}{s} - \frac{d}{2s} \left(\frac{\alpha_2 \psi\left(\frac{t_2 - u}{s}\right) + \alpha_1 \psi\left(\frac{t_1 - u}{s}\right)}{\alpha_2 \psi\left(\frac{t_2 - u}{s}\right) - \alpha_1 \psi\left(\frac{t_1 - u}{s}\right)} \right) \quad (6)$$

where $\bar{t} = \frac{t_1 + t_2}{2}$ and $d = t_2 - t_1$. It corresponds to a signal having two singularity points in t_1 and t_2 as depicted in Fig. 2. Each singularity does not change its location till it starts to interfere with the neighbouring one,

i.e. till their cones of influence do not overlap. In fact, $\psi(\frac{t_1-t_2}{s}) = 0$ if d is greater than the wavelet support at scale s . Moreover, the higher α_k the smaller the shift. In other words, the larger maximum quickly englobes the smaller one — see [3] for details.

The equations (6) and (19) can be solved using standard iterative methods for ode with suitable initial conditions. They consists of $\alpha_k s$ and $t_k s$ computed at $s = 1$ using the algorithm described in the previous section. Choosing a wider set of atoms, for example the family of infinite polynomial ramps, the equation becomes more general while the class of well approximated functions is enlarged. Nonetheless, it would also include the estimation of growing exponent of each α_k , since polynomial functions of different degrees are considered [3]. Hence, the amount of information to code, along with iterative schemes for solving the equation make it directly not useful for a compression scheme. On the other hand, in general the law cannot be inverted: it predicts coefficients from finer to coarser scale, while it is not possible the opposite, except for not completely interfering waves. In other words, if two waves are interfering but their atoms are still distinguishable, one can predict their location and amplitude in a previous scale. On the contrary, one cannot say anything about their origin for complete interfering waves, as happens in [5].

Nonetheless, the law combined with the atomic decomposition guarantee a strong and precise relation between maxima at successive scales. This dependence can be translated in a relation between low pass and high pass components at the same scale. In fact, for small increments Δs of the scale parameter, atoms locations for $Wf(u, s)$ are close to the ones at $Wf(u, s + \Delta s)$ (see eqs. 6 and 19). On the other hand, using the wavelet decomposition into low and high pass components, $Wf(u, s + \Delta s)$ can be derived from the approximation band $A(u, s)$ at scale s . In the next section we show how to exploit information in the low pass component for predicting the high pass one at the same scale.

IV. A PROPOSAL FOR COMPRESSION

In this section we propose a practical way for exploiting previous results for compression purposes. In particular, we will see that the coder will send just low pass information, since the decoder will be able to also predict wavelet details. This is possible thanks to the main peculiarity of WISDOW that approximates any kind of singularity via the atom shown in Fig. 1b.

For the sake of simplicity, suppose to have a signal with just one singularity. We will consider an overcomplete dyadic wavelet decomposition, i.e. $s = 2^j$, computed up to J^{th} level using biorthogonal filters $\{\phi, \psi, \tilde{\phi}, \tilde{\psi}\}$. ϕ and ψ are respectively the low and high pass analysis filters while $\tilde{\phi}$ and $\tilde{\psi}$ are the corresponding synthesis filters. Let us indicate the coarsest (low pass) component of the decomposition with A_J while $\{D_j\}_{1 \leq j \leq J}$ are the details at level j . Suppose that we want to compute the low pass component at the finer scale A_{J-1} without using

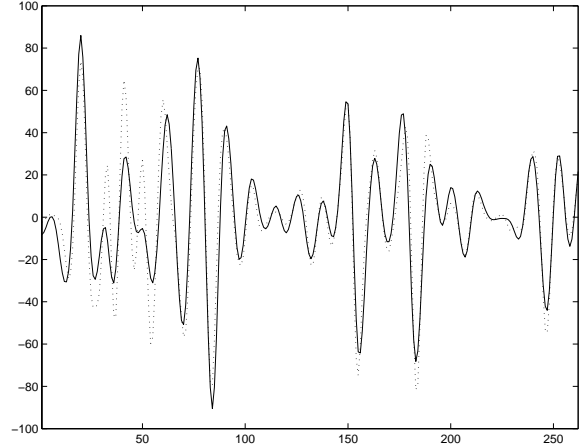


Fig. 11. Zoom of the estimated detail band (3^{rd} level) of column no. 100 of Lena image using the proposed algorithm. The dotted line depicts the original one while the solid line is the estimation.

the corresponding detail (high frequency) component D_J . Obviously, we will obtain only an estimate of A_{J-1} , that we will be indicated with \tilde{A}_{J-1} . More precisely:

$$\tilde{A}_{J-1} = A_J * \tilde{\phi}$$

where $\tilde{\phi}$ is the low pass synthesis filter of the adopted wavelet frame. Now, if we want to achieve A_J from \tilde{A}_{J-1} we have to perform the convolution with low pass analysis filter ϕ , that is

$$\tilde{A}_J = \tilde{A}_{J-1} * \phi = A_J * \tilde{\phi} * \phi. \quad (7)$$

Hence,

$$E_J = A_J - A_J * \tilde{\phi} * \phi, \quad (8)$$

is the error for the omission of the high pass information. The question now is: is it possible to recover the high pass information D_J from E_J ? The positive answer arises from the wavelet reconstruction formula:

$$A_{J-1} = A_J * \tilde{\phi} + D_J * \tilde{\psi},$$

where $\tilde{\psi}$ is the high pass synthesis filter. In fact, by convolving both members with ϕ , it holds

$$A_J - A_J * \tilde{\phi} * \phi = D_J * \tilde{\psi} * \phi. \quad (9)$$

Hence, comparing (9) and (8) we have

$$E_J = D_J * \tilde{\psi} * \phi. \quad (10)$$

On the other hand, the atomic decomposition provides

$$D_J(u, 2^J) = \alpha_0 F(t_0, u, 2^J)$$

where $F(t_0, u, 2^J)$ is eq. (3) computed at $s = 2^J$. Hence

$$E_J = \alpha F_J * \tilde{\psi} * \phi, \quad (11)$$

where $F_J = F(t_0, u, 2^J)$.

It is worth outlining that the biorthogonality condition

$$\hat{\phi}^*(\omega)\hat{\phi}(\omega) + \hat{\psi}^*(\omega)\hat{\psi}(\omega) = 2$$

guarantees a not trivial identity — the left side of (9) is non zero. It turns out that $F_J * \tilde{\psi} * \phi$, which is depicted in Fig. 9, represents a basic atom for E_J . It is characterized by the location of its modulus maximum and its amplitude is regulated by the slope α . More in general, if D_J is the detail band of a generic signal, the atomic decomposition provides

$$D_J(u, 2^J) = \sum_k \alpha_k F(t_k, u, 2^J)$$

and then

$$E_J(u, 2^J) = \sum_k \alpha_k F(t_k, u, 2^J) * \tilde{\psi} * \phi.$$

Moreover, each $F(t_k, u, 2^J) * \tilde{\psi} * \phi$ preserves maximum location of $F(t_k, u, 2^J)$ — see Fig. 9. An example of how E_J is strongly correlated to the detail band D_J is shown in Fig. 10.

The recovering algorithm is straightforward. For each significant maximum t_k of E_J , the corresponding slope α_k can be estimated using eq. (11) as model function and the expansion algorithm described in Section II. The couples $\{(t_k, \alpha_k)\}$ also characterize atoms in D_J . Then, at each t_k a wavelet basic atom $F(t_k, u, 2^J)$ (eq. (3)) with slope α_k is modelled and each contribution is suitably summed exploiting the *overlapping effects principle*. An example of the reconstructed detail band is depicted in Fig. 11. A step backward of the transform can be now performed and the algorithm is iterated till the first scale is reached.

The residual information E_J can be caught only in a wavelet frame decomposition since its overcompleteness. Unfortunately, this would imply to carry on the undecimated approximation band of the wavelet decomposition. Nonetheless, time frequency decomposition of the wavelet transform allows us to describe the approximation band by means of its first $\frac{M}{2^J}$ DCT (Discrete Cosine Transform) coefficients, since it represents the frequency contribution for the J^{th} level of the wavelet transform while M is the signal length. Indeed, the not perfect cut off frequency of the adopted filters could require few additional components of the DCT. Fig. 12 depicts the low pass component of a signal and its approximation using the first $M/2^j$ coefficients of its discrete cosine transform ($SNR = 48.68$ db). As it arises from the figure, the two signals are very close.

A. The Algorithm

In the following the coding and decoding algorithms for a single signal will be given. Let M be the signal length.

Coder

- 1) Perform the undecimated discrete wavelet transform (UDWT) up to J^{th} level of the analysed signal.
- 2) Perform the DCT of the coarsest approximation band.
- 3) Extract the first $\frac{M}{2^J}$ coefficients of DCT and indicate the resulting vector with V .

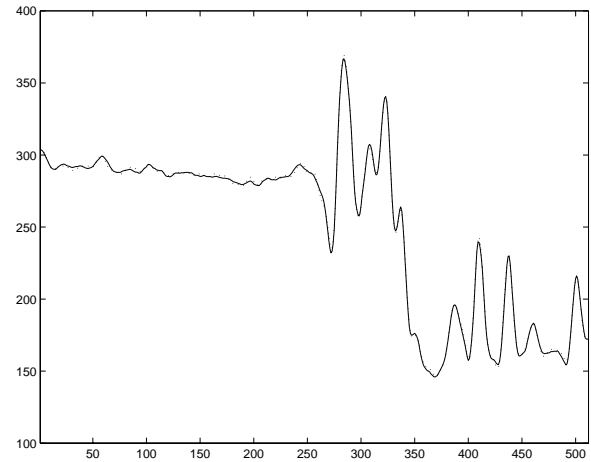


Fig. 12. Low pass component at 3^{rd} scale level of the row no. 100 of Lena image (solid line) its approximation using the first 64 coefficients of the DCT (dotted line)— SNR = 48.68 db.

- 4) Uniformly quantize and entropy code them — Huffman coding is used.

Decoder

- 1) Dequantize and reconstruct the UDWT approximation band A_J by inverting the DCT transform, padding the vector V with zeros to length M before transforming.
- 2) Using A_J , perform a step backward of the UDWT transform using the low pass synthesis filter $\check{\phi}$.
- 3) From the output of step 2, perform a step forward of the UDWT transform using the low pass analysis filter ϕ , as in eq. (7).
- 4) Compute the difference between A_J and the output of step 3 and perform the high pass synthesis filter ψ . This filtering operation is done just for emphasizing atoms' shapes.
- 5) From the output of step 4, estimate significant maxima locations t_k and their corresponding α_k s using the left side of eq. (11) and the algorithm in Section II.
- 6) In correspondence of each t_k , model the basic atom (3) whose slope is α_k and sum each contribution to obtain the detail band D_J at J^{th} level.
- 7) Perform a step of the inverse UDWT to obtain A_{J-1} .
- 8) Put $J = J - 1$ and repeat steps 2 to 7 till the first (finest) scale level is reached.

As we mentioned in the Introduction, the evolution law and atomic approximation are well defined for 1D signals. For that reason, authors' choice has been to independently process each column of an image in order to exploit 1D results. It is obvious that other choices are possible. Nonetheless, since the adopted representation strongly depends on WISDOW approximation, it is reasonable to choose the direction yielding better performances.

V. EXPERIMENTAL RESULTS

The algorithm has been tested on different signals and images. In this section, we give some results achieved on

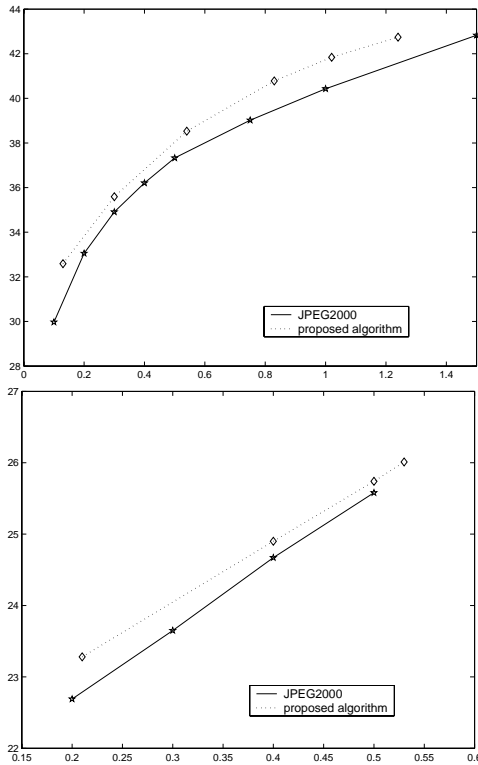


Fig. 13. rate-distortion curves (PSNR versus bpp) of the proposed compression scheme and standard JPEG2000 for Lena image (top) and Baboon image (bottom).

$512 \times 512 \times 8\text{bits}$ Lena and Baboon images. As mentioned in the previous section, results depend on WISDOW approximation and on the number of completely interfering atoms. For that reason, a three scale level UDWT has been employed. Spline biorthogonal wavelets having 3/9 filters length have been used in all experiments. They are particularly useful since their corresponding basic atoms are easily recognizable, making the algorithm simpler. With regard to images, performances are influenced by the adopted 1D decomposition. For example, Lena image has been processed by columns while Baboon by rows. Even if for Lena image results slightly change, for Baboon the gain is about 1 db since its symmetry.

With regard to quantization, a uniform one can be roughly used for DCT coefficients. Nonetheless, it can be slightly improved by choosing non uniform quantization steps depending on the amplitude of coefficients — the average gain is 0.4db in terms of PSNR (*Peaked Signal to Noise Ratio*). In the experiments we used the JPEG quantization table expanded to $M/2^j$ blocks, where M is the image size. In other words, more bits are allocated for high value coefficients, while for the others the number of bits decreases according to their amplitude. The quantized coefficients are entropy coded using Huffman algorithm.

Even in a very rough implementation, achieved results are quite promising, as shown in Fig. 13, where rate-distortion curves of the proposed algorithm and standard JPEG2000 are depicted. Comparisons with JPEG are omitted since the latter is outperformed by JPEG2000. In

Fig. 14, compressed Lena ($\text{bpp} = 0.3$, $\text{PSNR} = 35.59\text{db}$) and Baboon ($\text{bpp} = 0.4$, $\text{PSNR} = 24.90\text{db}$) images are shown. It is worth highlighting that for completely interfering atoms it is impossible to separate single contributions, as theoretically proved in Appendix B. In this case, it is necessary to code α_k s estimation error for decreasing the distortion. To this aim the coder has to work as the decoder and compute the difference between the estimation of α_k from the detail band using WISDOW and the one from E_J using the proposed scheme. This error can be then uniformly quantized and stored. During the decoding phase, it is de-quantized and added to each α_k after its estimation in step 5 of the decoding algorithm in Section IV.A. For each band the storage of α_k estimation error is not expensive since the sparseness of the atomic representation. Nonetheless it is required since the decoding algorithm is progressive and than it is subject to the propagation of errors computed at coarsest scales.

We also perform some experiments by processing non overlapping blocks 16×16 of the image expanding them in a circular manner (see Fig. 15). Achieved results are comparable to the ones achieved by processing the images by rows or columns, as shown in Fig. 16. These results confirms that the atomic approximation is a crucial step in the proposed compression scheme, as stated in the last paragraph of Section IV.A.

Finally, the algorithm is fast and computationally not expensive, since it requires simple filtering operations. Moreover, the splitting of each wavelet band into independent atoms allows us to provide a representation by maxima of the wavelet transform and then a fast and simple signal reconstruction.

VI. CONCLUSIONS

In this paper, an algorithm for signal and image compression has been presented. It is an attempt to avoid the numerical resolution of the travelling law for modulus maxima coefficients of the wavelet transform of a generic signal. In fact, from the equation regulating the wavelet transform of a given function, it is possible to derive a rule for constructing maxima chains along scales of the transform. In its general version, the proposed equation generalizes time scale laws for wavelet coefficients presented in [7] and [5]. Nonetheless, it becomes easier to solve it if some approximations of the signal are assumed. In particular, a decomposition in single atoms of the wavelet transform noticeably simplifies the equation, making it easier to manage. Although powerful, the equation requires too many initial conditions for being solved and then embedded in a compression scheme. For that reason, a combination of filtering operations has been proposed. It is oriented to achieve a set of oracle data that allows us a suitable atomic decomposition. Each atom predicts both the location and α value of the corresponding one in the detail band. Future research will consist of improving the reconstruction algorithm along



Fig. 14. Compressed Lena image (top) at 0.3 bpp and 35.59 db and Baboon image (bottom) at 0.4 bpp and 24.90 db using the proposed compression scheme.

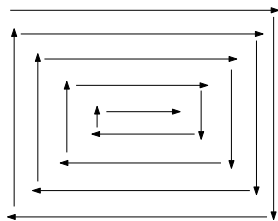


Fig. 15. Each block of the image can be expanded into a 1D signal following a circular direction as shown in the Figure.

with a deeper investigation of further potentialities of the evolution laws.

APPENDIX A

STEP FUNCTIONS AND INTERFERING ATOMS

Proposition 1: Let f_t be a discontinuous function in t_1 , that is

$$f(t) = \begin{cases} \alpha & t < t_1 \\ \gamma & t \geq t_1 \end{cases}$$

and let $f_1(t)$ be a finite ramp function defined as follows

$$f_1(t) = \begin{cases} \alpha & t < t_1 \\ \alpha_1 t + \beta & t_1 \leq t < t_2 \\ \gamma & t \geq t_2 \end{cases}$$

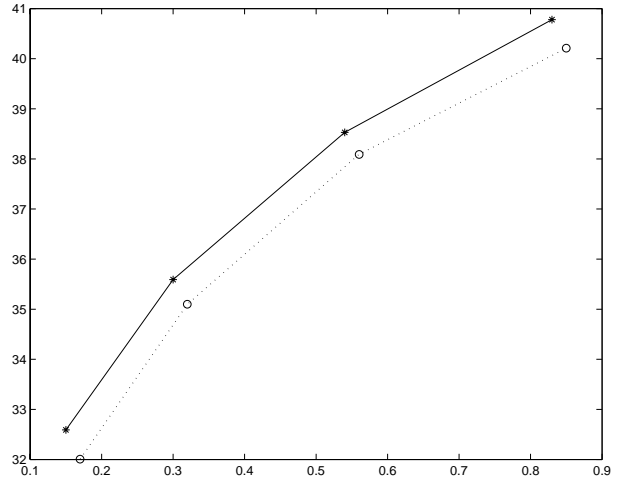


Fig. 16. PSNR versus bpp results for Lena image achieved by the proposed compression scheme. Solid line corresponds to column by column processing while dotted line refers to the circular blocks

where $\alpha = \alpha_1 t_1 + \beta$ and $\gamma = \alpha_1 t_2 + \beta = \alpha_1(t_2 - t_1) + \alpha$. The wavelet transform of f is the limit of the wavelet transform of f_1 , when t_2 approaches t_1 .

Proof:

$$W f_1(u, s) = \frac{1}{\sqrt{s}} \left\{ \int_{u+sa}^{t_1} \alpha \psi \left(\frac{t-u}{s} \right) dt + \int_{t_1}^{t_2} (\alpha_1 t + \beta) \psi \left(\frac{t-u}{s} \right) dt + \int_{t_2}^{u+sb} \gamma \psi \left(\frac{t-u}{s} \right) dt \right\}.$$

Using the change of variable $y = \frac{t-u}{s}$, the continuity conditions for the function f_1 and the zero mean property of the wavelet ψ , we have

$$W f_1(u, s) = s\sqrt{s} \left\{ \int_{\frac{t_1-u}{s}}^{\frac{t_2-u}{s}} \alpha_1 y \psi(y) dy - \alpha_1 \frac{t_1-u}{s} \int_{\frac{t_1-u}{s}}^{\frac{t_2-u}{s}} \psi(y) dy + \alpha_1 \frac{t_2-t_1}{s} \int_{\frac{t_2-u}{s}}^b \psi(y) dy \right\}. \quad (12)$$

Since $\gamma = \alpha_1(t_2 - t_1) + \alpha$, then $\alpha_1(t_2 - t_1) = \gamma - \alpha$. Therefore, the last term of the previous equation becomes

$$\frac{\gamma - \alpha}{s} \int_{\frac{t_2-u}{s}}^b \psi(y) dy.$$

Hence

$$\lim_{t_2 \rightarrow t_1} W f_1(u, s) = \sqrt{s}(\gamma - \alpha) \int_{\frac{t_1-u}{s}}^b \psi(y) dy,$$

which is the wavelet transform of the function $f(t)$.

□

APPENDIX B
EVOLUTION LAWS OF WAVELET ATOMS

Let ψ be a wavelet function such that $\bar{\psi} = \frac{1}{\sqrt{s}}\psi(-\frac{u}{s})$. By computing its partial derivatives with respect to the variables u and v , the following PDE [6] can be written

$$\frac{\partial}{\partial s}\bar{\psi} = \frac{\partial}{\partial u}\left(-\frac{u}{s}\bar{\psi}\right) + \frac{1}{2s}\bar{\psi}.$$

Hence, by convolving each side of the previous equation with f , it follows

$$\frac{\partial}{\partial s}Wf(u, s) = \frac{\partial}{\partial u}\left(f * \left(-\frac{u}{s}\bar{\psi}\right)\right) + \frac{1}{2s}Wf(u, s). \quad (13)$$

If f is the infinite ramp signal in (1), the term $\frac{\partial}{\partial u}\left(f * \left(-\frac{u}{s}\bar{\psi}\right)\right)$ can be developed and with a bit of calculations eq. (13) becomes

$$\frac{\partial}{\partial s}Wf(u, s) = \frac{t_0 - u}{s}\frac{\partial}{\partial u}Wf(u, s) + \frac{3}{2s}Wf(u, s). \quad (14)$$

This represents the evolution law through scales of an isolated atom in the wavelet domain. Under regularity assumptions, one can perform the derivative with respect to u on both sides of eq. (14), that is

$$\begin{aligned} \frac{\partial}{\partial s}\frac{\partial}{\partial u}Wf(u, s) &= -\frac{1}{s}\frac{\partial}{\partial u}Wf(u, s) + \\ &+ \frac{t_0 - u}{s}\frac{\partial^2}{\partial u^2}Wf(u, s) + \frac{3}{2s}\frac{\partial}{\partial u}Wf(u, s). \end{aligned} \quad (15)$$

Let $\bar{u}(s)$ be the maxima curve along scale, for $u = \bar{u}(s)$ previous equation becomes

$$\frac{\partial}{\partial s}\frac{\partial}{\partial u}Wf(s, \bar{u}(s)) = \frac{t_0 - \bar{u}(s)}{s}\frac{\partial^2}{\partial u^2}Wf(s, \bar{u}(s)). \quad (16)$$

On the other hand, for a maximum point of $Wf(u, s)$ it holds

$$\frac{\delta}{\delta s}\left(\frac{\delta}{\delta u}Wf(s, \bar{u}(s))\right) = 0,$$

that is

$$\frac{\partial}{\partial s}\frac{\partial}{\partial u}Wf(s, \bar{u}(s)) + \frac{\partial^2}{\partial u^2}Wf(s, \bar{u}(s))\dot{\bar{u}} = 0. \quad (17)$$

By comparing (16) and (17), the following ode for $\bar{u}(s)$ is provided

$$\dot{\bar{u}} = \frac{t_0 - \bar{u}(s)}{s}. \quad (18)$$

For a signal having more than one singularity point, from the *overlapping effects principle* and the atomic decomposition, each singularity satisfies eq. (14). Hence, eq. (13) becomes

$$\begin{aligned} \frac{\partial}{\partial s}Wf(u, s) &= \frac{\bar{t}_0 - u}{s}\frac{\partial}{\partial u}Wf(u, s) + \frac{3}{2s}Wf(u, s) + \\ &+ \frac{1}{Ns}\sum_{k=1}^N\left(\frac{\partial}{\partial u}w_u^{(k)}\left(\sum_{j=1}^N d_{kj}\right)\right) \end{aligned}$$

where $w_u^{(k)}$ is the first order partial derivative with respect to u of the k^{th} atom, $\bar{t} = \frac{\sum_{k=1}^N t_k}{N}$ and $d_{kj} = t_k - t_j$.

With analogous calculations, the following ode for maxima locations can be provided

$$\dot{\bar{u}} = -\frac{\bar{t} - \bar{u}}{s} - \frac{1}{Ns}\frac{\sum_{k=1}^N[w_{uu}^{(k)}(\sum_{j=1}^N d_{kj})]}{\sum_{k=1}^N w_{uu}^{(k)}}, \quad (19)$$

where $w_{uu}^{(k)}$ is the second order partial derivative with respect to u of the k^{th} atom, i.e. $w_{uu}^{(k)} = \frac{1}{\sqrt{s}}\alpha_k\psi\left(\frac{t_k - u}{s}\right)$.

The second term of the right side of the ODE regulates the shift of maxima locations with respect to their midpoint \bar{t} . The shift is weighted by the maximum α_k value and its closeness to the neighbouring ones. In fact, $\psi\left(\frac{t_k - u}{s}\right)$ are zero for d_{kj} greater than the support size of ψ at the analysed scale —see [3] for details.

REFERENCES

- [1] "Jpeg software codec," *Portable Res. Video Group, Stanford Univ., CA*, 1997.
- [2] V. Bruni and D. Vitulano, "Signal de-noising via overlapping atoms in a wavelet domain," *Proceedings of ISPA 2003*, pp. 459–464, September 2003.
- [3] —, "Scale space atoms for signals and image de-noising," *IAC Report - C.N.R.*, no. 86, February 2006.
- [4] —, "Wavelet based signal de-noising via simple singularities approximation," *Signal Processing*, vol. 86, pp. 859–876, April 2006.
- [5] P. Dragotti and M. Vetterli, "Wavelet footprints: Theory, algorithms and applications," *IEEE Trans. on Signal Processing*, vol. 51, no. 5, pp. 1306–1323, May 2003.
- [6] L. C. Evans, *Partial Differential Equations*. American Mathematical Society, 1999.
- [7] S. Mallat, *A Wavelet Tour of Signal Processing*. Academic Press, 1998.
- [8] S. Mallat and W. Hwang, "Singularity detection and processing with wavelets," *IEEE Trans. on Information Theory*, vol. 38, no. 2, pp. 617–643, March 1992.
- [9] S. Mallat and Z. Zhang, "Matching pursuits with time frequency dictionaries," *IEEE Transactions on Signal Processing*, vol. 41, no. 12, pp. 3397–3415, December 1993.
- [10] S. Mallat and S. Zhong, "Characterization of signals from multi-scale edges," *IEEE Trans. on PAMI*, vol. 14, no. 7, pp. 710–732, July 1992.
- [11] A. Said and W. Pearlman, "A new, fast and efficient image codec based on set partitioning in hierarchical trees," *IEEE Trans. on Circuits Syst. Video Technol.*, vol. 6, no. 3, pp. 243–249, June 1996.
- [12] J. Shapiro, "Embedded image coding using zero-trees of wavelet coefficients," *IEEE Trans. on Signal Processing*, vol. 41, pp. 3445–3462, December 1993.
- [13] B. Usevitch, "A tutorial on modern lossy wavelet image compression: Foundations of jpeg 2000," *IEEE Signal Processing Magazine*, pp. 22–35, September 2001.

Vittoria Bruni received the degree in Mathematics from the University of Rome "La Sapienza" in 2001. Her graduation thesis was in detection of line scratches on digital images. In January 2006 she received the PhD degree in applied mathematics from the University of Rome "La Sapienza", Department of Mathematical Methods and Models for Applied Sciences. Title of PdD Thesis: "A Wavelet based Model for Image Denoising and Compression". Her research interests include image compression, denoising and restoration, wavelets theory and applications, pattern recognition with applications in the Field of Cultural Heritage.

Since September 2001 she collaborates with the Institute for the Application of Calculus (IAC) of National Council of Research in Rome within national and international projects. She is currently supported by MIUR-FIRB project "A Knowledge based model for digital restoration and enhancement of images concerning archaeological and monumental heritage of Mediterranean Coast". She is currently lecturer at University of Rome "Tor Vergata", Department of Mathematics, degree in "Mathematical Models for Image and Signal Processing".

Domenico Vitulano received the physics degree from the University of Naples "Federico II" in 1993 and M. Sc. degree (summa cum laude) in information and communication technology from IIASS "R.R. Caianello" Institute of Vietri sul Mare, Salerno, in 1997. His research interests include pattern recognition, image and data compression, indexing and computer vision.

Since 1995 he is at Institute for the Application of Calculus of National Council of Research in Rome, where He has been involved in various national and international Research Projects concerning Cultural Heritage. He has been scientific responsible of section "Image Coding" of National Project "Researches and developments of Innovative Models for Investigation and Aided Diagnosis". He is currently lecturer at University of Rome "Tor Vergata", Department of Mathematics, degree in "Mathematical Models for Image and Signal Processing".

He is author and co-author of more than fifty scientific papers on journals, tutorials, monographs and proceedings of workshops. He is also referee for many International Journals and Conferences.

Benedetto Piccoli received the Laurea degree (cum laude) from the University of Padova, Italy, and the Ph.D. degree from the International School for Advanced Studies (SISSA/ISAS), Trieste, Italy, in 1991 and 1994, respectively. Currently, he is research director at the Istituto per le Applicazioni del Calcolo "Mauro Picone" of the C.N.R. He has published more than 80 papers in journals, books, and refereed conferences. He is editor in chief of Networks and Heterogeneous Media and he is in the editorial board of SIAM Journal on Control and Optimization, Journal of Dynamical and Control Systems and ESAIM Control Optimization and Calculus of Variation. His main research interests are in the fields of control theory and PDEs.